THE ASTROPHYSICAL JOURNAL, 324:1056–1067, 1988 January 15

ASTROPHYSICAL IMPLICATIONS AND OBSERVATIONAL PROSPECTS OF X-RAY POLARIMETRY

P. MÉSZÁROS
Pennsylvania State University
R. NOVICK
Columbia Astrophysics Laboratory
G. A. CHANAN
University of California, Irvine
M. C. WEISSKOPF
NASA/Marshall Space Flight Center
AND
A. SZENTGYÖRGYI
Columbia Astrophysics Laboratory
Received 1987 April 16; accepted 1987 June 22

ABSTRACT

X-ray polarimetry is a prime tool for investigating the physics of compact objects, which has not been adequately exploited thus far. However, current low-cost technology and modest launch requirements could provide a large number of positive observations with a sensitivity factor at least 100 times greater than 10 years ago. The amount of astrophysical information potentially to be gained from this is enormous. The introduction of polarimetric information (direction and degree) would bring a quantum jump in the parameter space used to investigate compact objects, from the current two (spectra and time variability) to four independent parameters that models need to satisfy. This should greatly improve our ability to discriminate between various possible models. Such observations could lead to an elucidation of the rotation-powered and accretion-powered pulsar radiation mechanisms, could help clinch the identification of black hole candidates, and could decide between thermal and nonthermal AGN radiation models, as well as pin down the geometry of the accretion flows in both galactic and extragalactic sources.

Subject headings: instruments — polarization — radiation mechanisms — X-rays: general

I. INTRODUCTION

X-ray astronomy has lived through an extremely fruitful first stage of exciting discoveries, followed by a second stage of characterization studies of such diverse objects as AGNs, bursters, SNRs, pulsars, black hole candidates, and others. The next generation of major X-ray missions will also certainly reveal new types of sources, as well as vastly increase the number of detections. Meanwhile, major gaps remain in our understanding of the physics of many of the objects discovered so far. Theoretical modeling can go only part way toward resolving such major issues as what is the type of accretion disk around various sources, if it is a disk, or what is the geometry of the emission region of pulsars, whether fan or pencil, and whether we really have discovered black holes. The real proof or disproof of various models of these objects must be based on very specific observations, aimed at elucidating the nature of the physical mechanisms. Such studies have been made in the past, but very much remains to be done, and this need not await the launch of the major missions of the next decade. Many of these issues can be resolved with smaller missions which can be flown in the near future at modest cost.

For the most part, the physical analysis of compact X-ray sources has dealt with the properties in a two-parameter space, consisting of spectral characteristics and time variabilities. As we know, this parameter space is restricted enough that it allows often two or three quite different models to explain the observations successfully. What we need is to increase the parameter space, in order to discriminate better between different models. Imaging, which might provide badly needed extra information, is very useful for extended sources, but unfortunately it is not suited for the study of compact objects. A doubling of the observational parameter space from the present two (frequency and time) to four, however, is definitely feasible. It is possible to add the two extra dimensions provided by X-ray polarimetry, namely the direction and magnitude of polarization, to the previous two parameters. This would be currently, and for the near future, our most direct way of seeking a quantum leap in our understanding of the nature and structure of compact objects. With the launch of the major missions of the next decade, our understanding of the mechanism of operation of such high-energy sources as neutron stars and black holes could remain severely hampered if we lacked all information on the X-ray polarization. The inclusion of such capabilities in these missions is strongly desirable, as well as feasible. However, it is not necessary for the astrophysical community to wait for the launching of large missions to acquire this information; significant progress in this direction could also be achieved with current technology, and with available, low-cost rocket launchers, as described in § V.

The great importance of X-ray polarization measurements for astrophysics has been emphasized before (cf. Rees 1975). A number of theoretical calculations on various types of X-ray

sources (such as oblate scattering nebulae, accretion disks, SNRs, accreting pulsars, etc.; cf. Angel 1969, Gnedin and Sunyaev 1974; Lightman and Shapiro 1976; Pavlov and Shibanov 1979; Connors, Piran, and Stark 1980, and others) have indicated that significant polarization can be expected in many sources, and that this would give valuable information on the structure of the emission region. To date only a few such observations have been carried out. The most valuable result so far has been the detection of X-ray polarization ($P = 19\%$ at the 18 σ level) in a diffuse source, the Crab Nebula (Novick *et al.* 1972; Weisskopf *et al.* 1976, 1978). Observations by the same group on compact sources with the polarimeter aboard *OSO 8* have yielded marginally significant detections in Cyg X-1 (3% at 2.6 keV; Silver *et al.* 1978), and weak upper limits for the mean polarization (averaged over all pulse and binary phases) for the rotation-powered pulsar in the Crab (19% at 2.6 keV), and for the accretion powered pulsars Her X-1 (60%) and Cen X-3 (14%), Silver *et al.* (1979). These upper limits are compatible with theoretical values, but the measurements were not sensitive enough to achieve a meaningful comparison with theory. With currently achievable values of the sensitivity, which are a factor 100 better than for the *OSO 8* instrument (see § V) one should easily be able to measure the pulse phase dependence of the direction angle and polarization degree, which can be as high as 60%–70% (§ II).

In this paper we emphasize the pivotal role that can be played by X-ray polarization in discriminating between various theoretical models of X-ray emitting neutron stars and black holes, both galactic and extragalactic. We present the results of detailed calculations of the phase dependence of the polarization properties of accreting pulsars (§ II) and of accretion disks around unmagnetized neutron stars and black holes (§ III), and discuss briefly some other sources where polarization would be expected (e.g., AGNs, radio pulsars) in § IV. Some of the observational possibilities are treated in § V, where we discuss two possible (although by no means unique) types of instrument: a high-sensitivity, low-cost rocket-launched polarimeter system and a more powerful and versatile device, which may be flown on one of the larger platforms. Such instruments would have the ability to answer some of the key questions of contemporary high-energy astrophysics.

II. POLARIZATION STRUCTURE OF ACCRETING X-RAY PULSARS

In this section we calculate for simple accreting X-ray pulsar models the expected degree of polarization and the electric vector position angle as a function of the spin phase. We use the generic pencil beam and fan beam accretion column models considered by Mészáros and Nagel (1985*b*). In the former, the radiation escapes predominantly along the magnetic axis, and in the latter, predominantly perpendicular to it. The geometrical configuration is depicted in Figure 1. Aside from orbital effects, the neutron star spin angular momentum is considered to be fixed in space, and the viewing angles i_1 and i_2 represent, respectively, the inclination between the angular momentum $\boldsymbol{\Omega}$ and the wave vector $\boldsymbol{k}$ (or the observer), and the inclination between the angular momentum $\boldsymbol{\Omega}$ and the stellar magnetic field $\boldsymbol{B}$. The plane of the sky is indicated by the axes u and v, so that the angle between $\boldsymbol{\Omega}$ and u is $\pi/2 - i_1$. The sky-projection of the angular momentum vector $\boldsymbol{\Omega}_\perp$ coincides with u, and the projection of the magnetic vector $\boldsymbol{B}_\perp$ makes an angle β with the axis u, with positive angles measured counterclockwise.

a) Polarization Quantities

The angle β oscillates about u as a function of the spin phase ϕ, according to

$$\beta = \tan^{-1}\left[\frac{-\sin(i_2)\cos(2\pi\phi)}{-\sin(i_2)\cos(i_1)\cos(2\pi\phi) + \cos(i_2)\sin(i_1)}\right], \tag{1}$$

where the minus sign in the numerator makes β positive in the counterclockwise sense. The radiation has two normal polarization modes, ordinary (here labeled 1) and extraordinary (here labeled 2). The polarization convention is that used by Mészáros and Nagel (1985*a*, *b*), in which at low frequencies (where vacuum effects become negligible) the ordinary polarization ellipsoid 1 has its major axis at an angle χ_1 (mostly close to zero) with respect to the sky-projected stellar magnetic field $\boldsymbol{B}_\perp$, and the major axis of the extraordinary ellipsoid makes an angle χ_2 with respect to $\boldsymbol{B}_\perp$ (mostly close to 90°). At higher frequencies, if vacuum effects dominate, the character of 1 and 2 are interchanged. This 1, 2 convention is opposite to the usual one, but it is kept here for consistency with previous calculations. With respect to the fixed direction of $\boldsymbol{\Omega}_\perp$, or the axis u, the major axes of the ellipsoids (which indicate the direction of the linear polarization for that mode) make angles of

$$\chi_1{}^u = \beta + \chi_1\,, \quad \chi_2{}^u = \beta + \chi_2\,, \tag{2}$$

in the plane of the sky.

The angles χ_j and the ellipticities of the normal modes are a function of the photon propagation angle θ with respect to the stellar magnetic field $\boldsymbol{B}$. Since the latter rotates in space, we have

$$\cos(\theta) = \cos(i_1)\cos(i_2) + \sin(i_1)\sin(i_2)\cos(2\pi\phi)\,. \tag{3}$$

The Stokes parameters of the observed radiation are related to the normal mode intensities I_1 and I_2 through

$$I = \sum_{j=1}^{2} I_j\,, \quad Q = \sum_{j=1}^{2} p_{Q_j} I_j\,, \tag{4}$$

$$U = \sum_{j=1}^{2} p_{U_j} I_j\,, \quad V = \sum_{j=1}^{2} p_{V_j} I_j\,, \tag{5}$$

cf. Gnedin and Pavlov (1974). The quantities p_{Q_j}, p_{U_j}, and p_{V_j} depend on the ellipticities and polarization angles of the normal modes, being functions of the magnetic field stength, frequency, density, and propagation angle. In a pulsar magnetic field, the strong birefringence causes the latter two Stokes parameters to average out to zero for a finite wave train, because the phase oscillates many times within the observation bandwidth as the radiation propagates outward; cf. Chanan, Novick, and Silver (1979). Thus, one expects only the linear polarization to survive, and this is given by the second of equations (4). The amplitude of linear polarization is given by

$$P_L = \frac{Q}{I} = \frac{\sum_{j=1}^{2} P_{Q_j} I_j}{\sum_{j=1}^{2} I_j}\,, \tag{6}$$

and the angle χ of the observed linear polarization (the electric vector) is given by the position angle $\chi_j{}^u$ (cf. eq. [2]) of the normal intensity I_j which is dominant at that frequency and angle, as given by a detailed radiative transfer calculation. For the latter we use the results of Mészáros and Nagel (1985*b*). Thus, if one knows I_1 and I_2 as a function of ω and θ, it is sufficient to calculate the quantities p_{Q_j} and $\chi_j{}^U$.

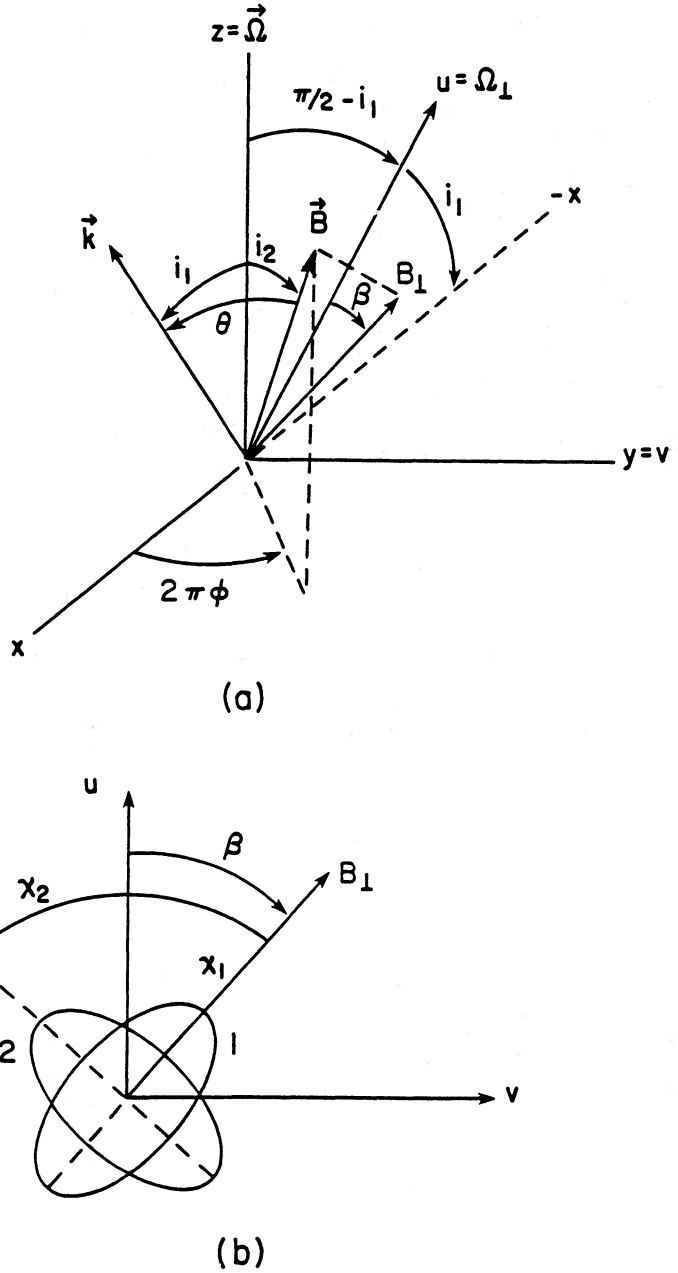

FIG. 1.—(*a*) Sketch of the geometrical configuration in space. The spin angular momentum $\boldsymbol{\Omega}$ coincides with z, the photon propagation direction to the observer $\boldsymbol{k}$ lies in the x, z plane, at an angle i_1 respect to $\boldsymbol{\Omega}$, or z, and at an angle θ respect to the stellar magnetic field $\boldsymbol{B}$. The angle between $\boldsymbol{B}$ and $\boldsymbol{\Omega}$, or z, is denoted i_2, and $\boldsymbol{B}$ has a phase angle $2\pi\phi$ respect to the x axis, ϕ being the usual phase. The plane of the sky perpendicular to $\boldsymbol{k}$ is obtained by rotating around y through $-(\pi/2 - i_1)$, and is denoted by the axes u, v. The projection of $\boldsymbol{\Omega}$ on the sky plane, $\Omega_\perp$, coincides with u, while the sky projection of $\boldsymbol{B}$, $B_\perp$ is at an angle β respect to u. (*b*) The sky plane u, v, showing the position of $B_\perp$ and the orientation of the normal mode polarization ellipsoids. The ordinary mode 1, when vacuum effects are negligible, is close to parallel to $B_\perp$, while the extraordinary 2 is close to perpendicular to it. When vacuum effects are important, the angles of 1 and 2 are interchanged.

b) Hot Plasma Normal Modes with Dissipation

In general, the normal mode structure is determined by the complex quantity α_j, cf. Gnedin and Pavlov (1974) and Bussard *et al.* (1987),

$$\alpha_j = r_j \exp(2i\chi_j) . \tag{7}$$

This is related to the complex parameter $b = q + ip = \text{cotan}(2\psi)$ through

$$\alpha_j = -b^{-1} \pm (1 + b^{-2})^{1/2} . \tag{8}$$

In the hot plasma limit with vacuum effects, b is given in Mészáros and Nagel (1985*a*) by

$$b = \frac{\sin^2\theta}{2\cos\theta} \frac{T_- + T_+ - 2T_z}{T_- - T_+} , \tag{9}$$

where the $T_{+,-,z}$ are components of the polarization tensor; cf. also Pavlov, Shibanov, and Yakovlev (1980), Kirk (1980), and Herold, Ruder, and Wunner (1981). For a general complex α_j,

the appropiate expressions for the p_{Q_j} and χ_j are

$$p_{Q_j} = \frac{2\ \mathrm{Re}\ (\alpha_j)}{|\alpha_j|^2 + 1}, \qquad \chi_j = \frac{1}{2} \tan^{-1}\left[\frac{\mathrm{Im}\ (\alpha_j)}{\mathrm{Re}\ (\alpha_j)}\right], \tag{10}$$

cf. Gnedin and Pavlov (1974). In this case, the presence of the nonzero imaginary part implies also a departure from a strict orthogonality of the two normal mode ellipsoids, although over most frequencies and angles this effect is not large; cf. Soffel *et al.* (1983).

c) *Model Calculations*

We have used the normal mode intensities $I_j(\omega, \theta)$ calculated by Mészáros and Nagel (1985*b*) for simple models of accreting polar caps or hot spots (which lie flush on the stellar surface around the magnetic poles and produce a pencil beam emission pattern) and accreting columns (which are represented as cylinders sticking out of the stellar surface around the magnetic poles, and give a fan beam pattern). These examples (models B and C in the reference above) are for a cyclotron energy $\omega_c = 38$ keV, Thomson optical depth $\tau_T = 20$, and density $\rho = 0.5$ g cm^{-3}. We have calculated the quantity α_j of equation (7) using the same hot plasma mode routine that was used for the calculation of the intensities, and have derived the degree of linear polarization using equation (6). The direction of the net linear polarization electric vector χ is given by either χ_1", or χ_2", cf. equation (2), depending on whether I_1 or I_2 dominates at a particular frequency and direction, as given by the transfer calculation.

In Figures 2 and 3 we have plotted the results for the hot spot/slab (pencil beam model) and for the column (fan beam model). The five divisions from left to right are values calculated for different observers at various viewing angles (i_1/i_2), which are indicated along the top of the picture. The top five panels show the normalized pulse flux amplitude, the middle five panels show the degree of linear polarization P_L, and the bottom five panels show the net polarization angle χ. The abscissa is the spin phase ϕ.

Looking at Figures 2 and 3, the most striking fact is that very large degrees of linear polarization P_L are obtained, reaching up to 80%. For both these pencil and fan beam models, the maximum P_L values are near the resonance frequency (this is the sixth curve up from the bottom for each panel). In these models, this occurs because at high densities and large optical depths most photons are thermally produced, and the disparity between the opacities in the two modes leads to a preponderance of one polarization. The reversal of behavior in the degree of polarization between the lower frequencies (e.g., second from bottom) and intermediate (e.g., fifth from bottom) is that different polarization modes dominate the spectrum at low frequencies (where plasma modes dominate) and at intermediate frequencies below the cyclotron line (where vacuum modes are important; cf. Mészáros and Nagel (1985*a*). These calculations do not include the two-photon emission process (Bussard, Mészáros, and Alexander 1985). While this would change the spectral details for models less dense than those considered here, the qualitative polarization structure is expected to be similar, i.e., highly polarized. Other models, with varying density and optical depth, also lead to high polarizations; cf. Mészáros and Nagel (1985*a*). At least two effects may contribute to reduce the total observable polarization. The first is propagation effects outside the emitting atmosphere, in a region of varying density and magnetic field strength. The importance of this effect has been considered by Gnedin, Pavlov, and Shibanov (1978*b*) and found to be small under most reasonable conditions. A second effect which tends to partially depolarize the observed flux is general relativistic light bending, which mixes rays from regions with different polarization characteristics, cf. Riffert and Mészáros (1988). For neutron star radii $R \gtrsim 9$ km, or over two Schwarzschild radii for 1.4 solar masses, this effect may be estimated to lead to a depolarization of less than 20%, or less than about 10% for $R \gtrsim 13$ km.

In comparing the pencil and fan models of Figures 2 and 3, one sees that phase measurements of the linear polarization would allow a decisive test to distinguish between the two: in pencil models the absolute value of P_L (*middle five panels*) is generally minimum when the flux amplitude (*top five panels*) is maximum (at phase zero), whereas in fan models the absolute value of P_L is maximum when the flux amplitude is also maximum (here shown as phase 0.5, although observationally one defines phase zero to be wherever the intensity is maximum). Physically, this is because the two normal opacities at frequencies less than the cyclotron frequency tend to be more dissimilar at propagation angles transverse to $\boldsymbol{B}$ (as in fans) and less dissimilar at propagation angles close to longitudinal respect to $\boldsymbol{B}$ (as in pencils); cf. Canuto, Lodenquai, and Ruderman (1972), Gnedin, Pavlov, and Shibanov (1978*a*, *b*), Mészáros and Ventura (19778, 1979).

Looking now at the direction of the net electric vector χ (*bottom five panels*), one sees that if a particular normal mode intensity dominates at all angles for a particular frequency, either χ_1" or χ_2", the curves are symmetrical with a change of sign around phase 0 and 0.5. The curves for χ_1" and χ_2" are mostly 90° apart. When at a particular frequency there is a change in dominance from one mode to the other at different angles, χ jumps by 90° to the other normal mode curve, while the degree of linear polarization goes through zero at that phase. In the particular case where at some phase the line of sight points directly down the magnetic pole (as for the second panel from left, $[i_1/i_2] = [45/45]$), one observes at some phases a discontinuity in the polarization angle of 180°. This is not due to a change in dominance from one mode to the other, but rather to a discontinuous jump of the position angle β of the sky-projected stellar magnetic field vector $\boldsymbol{B}_\perp$. Such jumps would occur at intensity maxima for pencil beams, but at intensity minima for fan beams. The probability of looking straight down the pole, however, is estimated to be small in randomly selected objects.

A measurement of the phase dependence of the direction of polarization would also allow to distinguish between pencil and fan beams. It is seen from Figures 2 and 3 that, aside from the discontinous jumps discussed above, in the pencil models (Fig. 2) the angle χ goes from positive to negative at pulse maxima (phase 0. and 1.) and from negative to positive at pulse minima (phase 0.5). In fan models (Fig. 3) the situation is opposite, χ going from negative to positive at pulse maxima, and from positive to negative at pulse minima. In addition, one sees also that during one cycle, the curves for χ pass through zero twice, the rate of change being larger in one passage than in the other. For pencils, the fast change of χ through zero occurs at pulse maxima, while for fans it occurs at pulse minima. This is related to the fact that pencil models tend to give narrower pulse widths than fan models (Nagel 1981; Mészáros and Nagel 1985*b*).

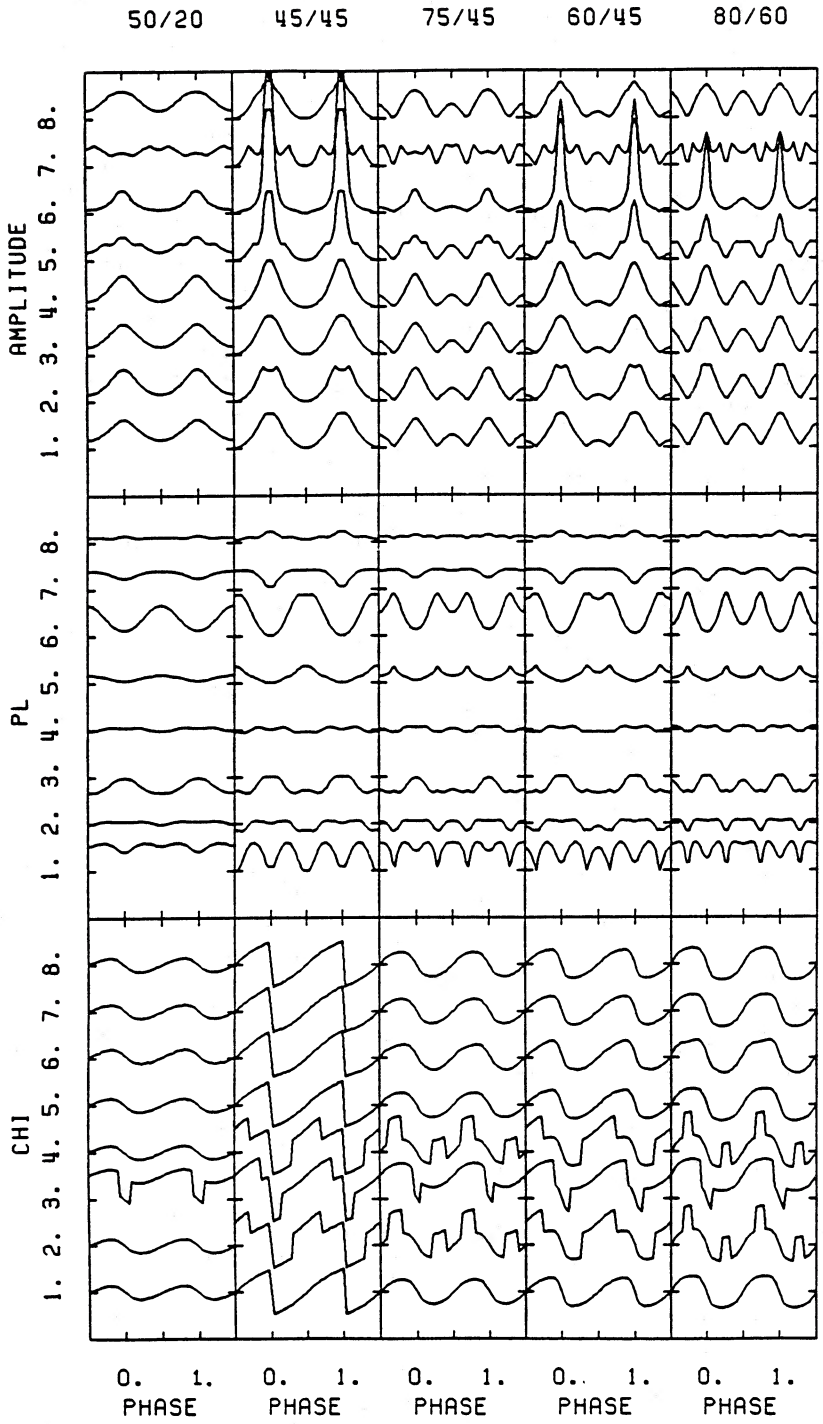

FIG. 2.—Pencil beam model, cyclotron energy $\omega_c = 38$ keV, $T = 8$ keV, $\rho = 0.5$ g cm^{-3} and $\tau_T = 20$. The pulse amplitude (*upper*), degree of linear polarization (*middle*), and polarization angle (*bottom*) are shown for eight frequencies. From bottom to top these are 1.6, 3.8, 9.0, 18.4, 29.1, 38.4, 51,7, and 84.7 keV, respectively. The cyclotron resonance is the sixth curve up. The pulse amplitude is normalized to the angle-integrated flux. The linear polarization goes from $+100\%$ to -100%, and the polarization angle goes from $+180°$ to $-180°$ ($\pm$one tick mark from the base mark for each curve). The five panels from left to right correspond to five choices of the viewing angles i_1/i_2, indicated along the top of the figure.

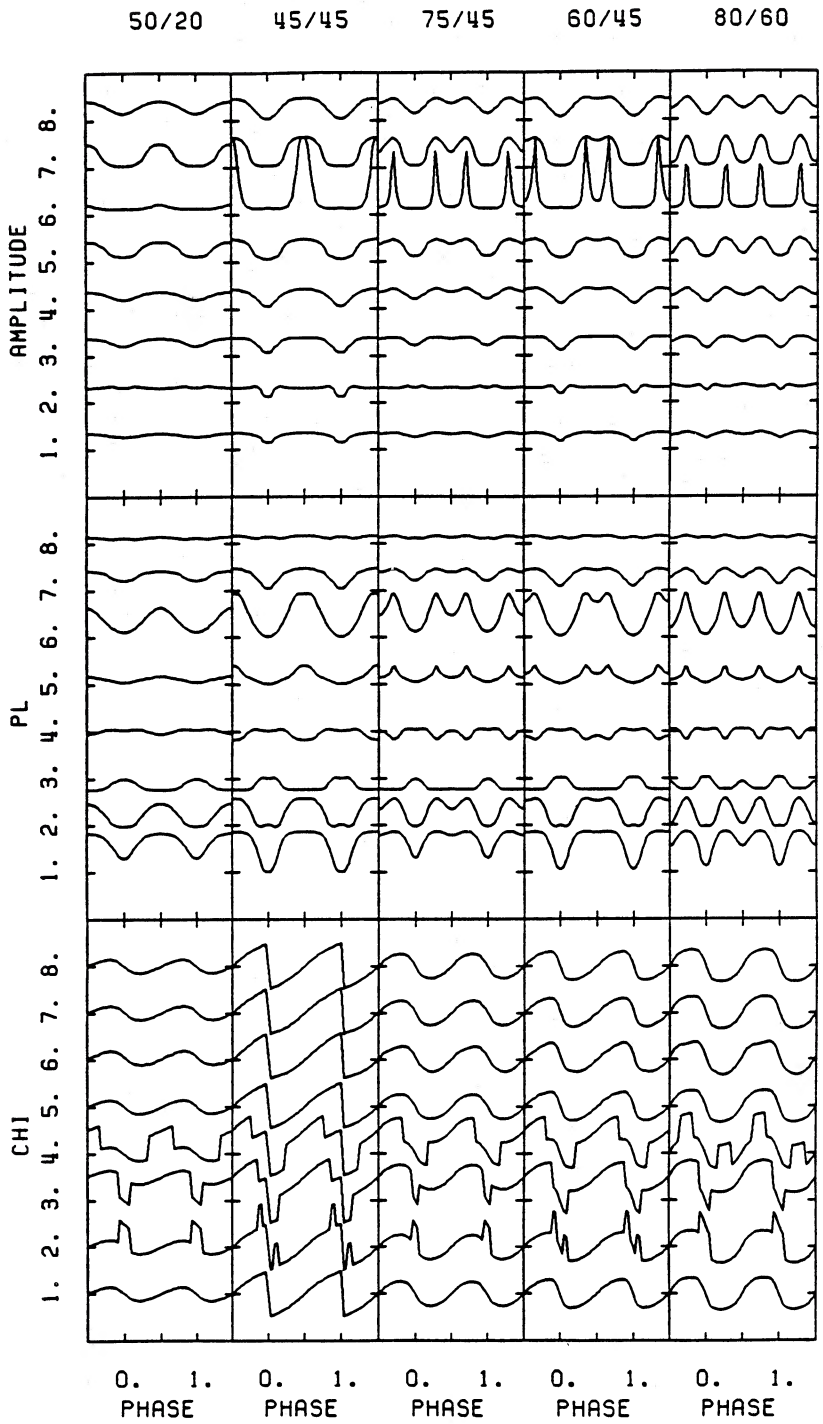

FIG. 3.—Fan beam model, same parameters and convention as in the previous Fig. 2

III. ACCRETION DISK POLARIZATION

The polarization expected from accretion disks has been discussed most recently by Phillips and Mészáros (1986), Sunyaev and Titarchuk (1985), and for the case of bursters by Lapidus and Sunyaev (1985). These papers also contain references to earlier work. The results of the above calculations show that the disk polarization is linear, with electric vector perpendicular to the symmetry axis of the disk for large scattering optical depths ($\gtrsim$few), and along the symmetry axis for small depths. The degree of polarization ranges from a maximum of $+11.7\%$ for large depths, to negative values in excess of -10% for low optical depths, where $(+, -)$ corresponds to an electric vector (perpendicular, parallel) to the symmetry axis. This applies to the case of disks where scattering is the dominant opacity, and the photons are of thermal origin, in which case the polarization is almost independent of frequency, for temperatures less than about 50 keV. If there is a

predominant source of low-frequency photons, then the high-energy Comptonized tail can have a larger degree of polarization. For disks around low magnetic field neutron stars, the boundary layer on the star contributes a significant fraction of unpolarized luminosity, and the expected degree of polarization is of the order of 2%–5%, while for accretion disks around Schwarzschild black holes, there is no stellar contribution and the larger values quoted above apply.

We shall use here as an example the case of high-luminosity accretion disks around a relativistic object, where the opacity is dominated by scattering. The disk is assumed to be plane parallel, the photon sources are distributed uniformly throughout its volume, and we assume that the central object does not contribute to the X-ray luminosity. The intensity and polarization as a function of angle are calculated with a Feautrier radiative transfer code described by Phillips and Mészáros (1986), and the results are shown in Figure 4. This gives the flux $F(\mu) = I(\mu)\mu$ normalized to its value at the surface normal ($\mu = 1$), and the degree of linear polarization P_L (%), as a function of the cosine of the angle respect to the disk normal, $\mu = \cos\theta$, the sign convention having been given above. The observed polarization and flux depend on both the optical depth (i.e., accretion rate), and the inclination angle at which the disk is observed. For a symmetry axis which is fixed in the sky over the duration of the observation (i.e., no disk precession), it suffices to know or estimate the optical depth τ_0 and the angular momentum vector of the disk to determine μ, and Figure 4 gives the degree and direction of polarization. One of the major contributions of X-ray polarimetry would be that it would allow one to investigate both the morphology of disk sources, aiding in the determination of the source orientation, and the internal physics of accretion disks, by pinning down the vertical depth for a given luminosity, which gives an estimate of the viscosity, or the α parameter.

Other systems where significant X-ray polarization is expected are galactic sources where the central source is

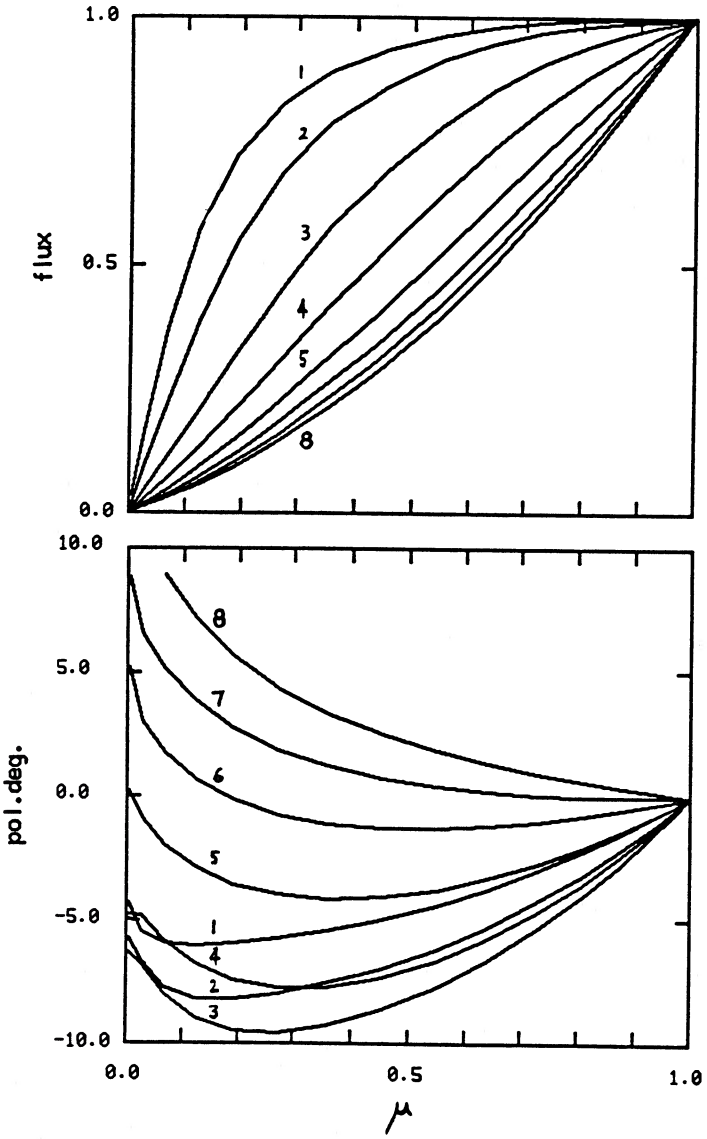

FIG. 4.—Accretion disk properties around an unmagnetized central object, with thermal sources uniformly distributed along its depth. (*top portion*) Flux $F(\mu) = I(\mu)\mu$ as a function of the cosine respect to the disk normal, μ, normalized to the value at $\mu = 1$, for the disk half-thickness $\tau_0 = 0.1, 0.2, 0.5, 1., 2., 4., 10., 100.$, numbered 1 through 8. (*bottom part*): Degree of linear polarization $P_L(\%)$, as a function of μ, for the same thicknesses as the top part.

believed to be blanketed by an accretion disk corona, which is itself optically thick to electron scattering, e.g., 4U 1822−37, 4U 2129+47 and Cyg X-3 (cf. Begelman and McKee 1983). In such models, the nearly sinusoidal modulation of the X-ray emission is due to the partial occultation of the corona by a bulge in the outer edge of the accretion disk, resulting from the interaction of the latter with the stream of incoming material from the companion star (White and Holt 1982). Another important application of polarimetry is its potential use as a tool for the discovery and investigation of precessing sources. Precessing X-ray disks have been considered in various contexts (Katz 1973; Roberts 1974; Petterson 1975; Rees 1975). Also, long time scale observations of some globular cluster sources (NGC 6441 and NGC 6624) as well as some bulge sources (4U 1916−05) show periodicities in the 100–200 day ranges which may be due to the presence of third companions (Grindlay 1985; Priedhorsky and Terrell 1984). One would expect this phenomenon to be associated with a change of the disk inclination angle respect to the observer, which could be proved by polarimetric measurements. This method should be applicable to sources where the disk contributes a significant fraction of the total luminosity, e.g., for weakly magnetized central objects (old neutron stars or black holes). The precession of disks around X-ray pulsars may not be detectable in the same way, since the disk contributes very little to the total X-ray luminosity. However, the possible precession of the magnetized neutron star itself (e.g., Her X-1; cf. Truemper *et al.* 1986) should be detectable, as an additional phase modulation of the X-ray pulsar polarization discussed in the previous section (i.e., the precession would be given by a periodic change in the angles i_1, i_2). Disk precession effects may be illustrated for several orientations of the total system angular momentum vector (which is fixed respect to the sky, and therefore respect to the observer), denoted by i_1, and the disk symmetry axis, which precesses around the system angular momentum vector and is at an angle i_2 with respect to this one. This is equivalent to our angles for the pulsar problem (eqs. [1]–[3]), where now the disk symmetry axis takes the role of $\boldsymbol{B}$, and the system angular momentum takes the role of the neutron star angular momentum Ω; cf. Figure 1. We show in Figure 5, for various values of the aspect angles i_1/i_2, the value of the flux (Fig. 5 [*top*]), the degree of polarization P_L (%) (Fig. 5 [*middle*]), and the electric vector angle χ with respect to the sky projection of the system angular momentum vector (Fig. 5 [*lower*]), as a function of the precession phase ϕ (for a nonprecessing disk, the "phase" represents just an arbitrary inclination of the disk respect to the plane of the sky). A measurement of the change of the degree of polarization would be an overwhelming proof of the precession of the disk, and a quantitative analysis, in comparison with model properties, could greatly increase our understanding of these sources.

General relativistic effects are generally weak for sources where the radiation propagates from and through distances greater than about three Schwarzschild radii from the compact object. This is thought to apply to many of the sources. Nonetheless, in some cases a significant fraction of the radiation may come from precisely those regions, and in this case some interesting general relativistic effects may be detected. The modifications on the total intensity have been discussed by Cunningham (1976), and Bardeen and Petterson (1975) have also considered the effects of both light-bending and distortion of the disk as a whole due to the dragging of inertial frames in a Kerr black hole. This latter effect tends to align the plane of the inner portion of the disk perpendicular to the hole's angular momentum, even if this is not parallel to the angular momentum of the accreted matter (as given, for instance, by the perpendicular of the binary orbital plane). Since the disk orientation can be determined by measuring the X-ray polarization, as described before, one may be able to detect a Kerr black hole if one observes a change in the direction of polarization from, say, the harder X-rays that originate closer in, and the softer X-rays originating further out (cf. Rees 1975). This could be particularly interesting in sources where a jet is present (e.g., Sco X-1, Cyg X-3, or SS 433) to give an independent handle on the angular momentum of (possibly) the innermost region. It would be even more interesting in quasars and AGNs, many of which have visible jets, where X-rays make up a significant fraction of their total luminosity. Even when an accretion disk is not distorted (e.g., a Schwarzschild black hole, or an aligned Kerr hole), the angle of polarization can suffer a gradual tilt away from purely parallel or perpendicular to the disk plane, for light rays traveling within a few Schwarzschild radii (Pineault 1977; Stark and Connors 1977; Connors, Piran, and Stark 1980). Thus, polarized light from a hot spot, say, would swing around significantly first in one sense and then in the other as the emitting spot passes behind the hole. There is also some demodulation of the degree of polarization, since the bending can mix light arising from regions of different initial polarization direction. While exact numerical predictions of these effects are strongly dependent on the (poorly understood) structure of the accretion flow within the last few Schwarzschild radii, the qualitative nature of the effects as described above, if detected, would be a signature of the presence of a relativistic object. If in addition one knew the mass to be greater than about three or four solar masses, the evidence for a black hole would be overwhelming.

IV. SOME OTHER X-RAY POLARIZATION SOURCES

We mention here, without attempt at detail or completeness, some other sources where X-ray polarimetry could bring about major advances in our understanding. The most promising from the feasibility point of view are the galactic sources, because of their higher observable flux. These would be definitely accessible to intruments such as those described in § V. Some extragalactic sources may also be measured by the simpler instruments, over a longer observing period. For extragalactic sources, however, reasonably short observing periods are achievable on the larger missions, equipped with grazing incidence photon collectors.

Foremost among the galactic sources would be the rotation-powered pulsars, which are expected to contain very strong magnetic fields (whose magnitude, unlike in some accreting pulsars, is not measured but inferred to be of order 10^{12} G). Because of this very strong field, just as in accreting pulsars, one expects the X-ray emission to be significantly polarized. The radio emission amounts to a trivial fraction (typically 10^{-5}) of the total inferred rotational energy loss, most of the energy coming out in the X-ray and gamma-ray ranges. These photons carry information on the particle acceleration and on the structure of the magnetosphere. So far five radio pulsars have been detected in the X-ray range, three pulsed (the Crab, MSH 15−25, and 0540−69) and two nonpulsed (Vela and PSR 1929+10), e.g., Taylor and Stinebring (1986). About a dozen or so diffuse X-ray nebulae have been detected, which are probably energized by pulsars within them (e.g., Helfand 1984). These are presumably emitting by the synchrotron

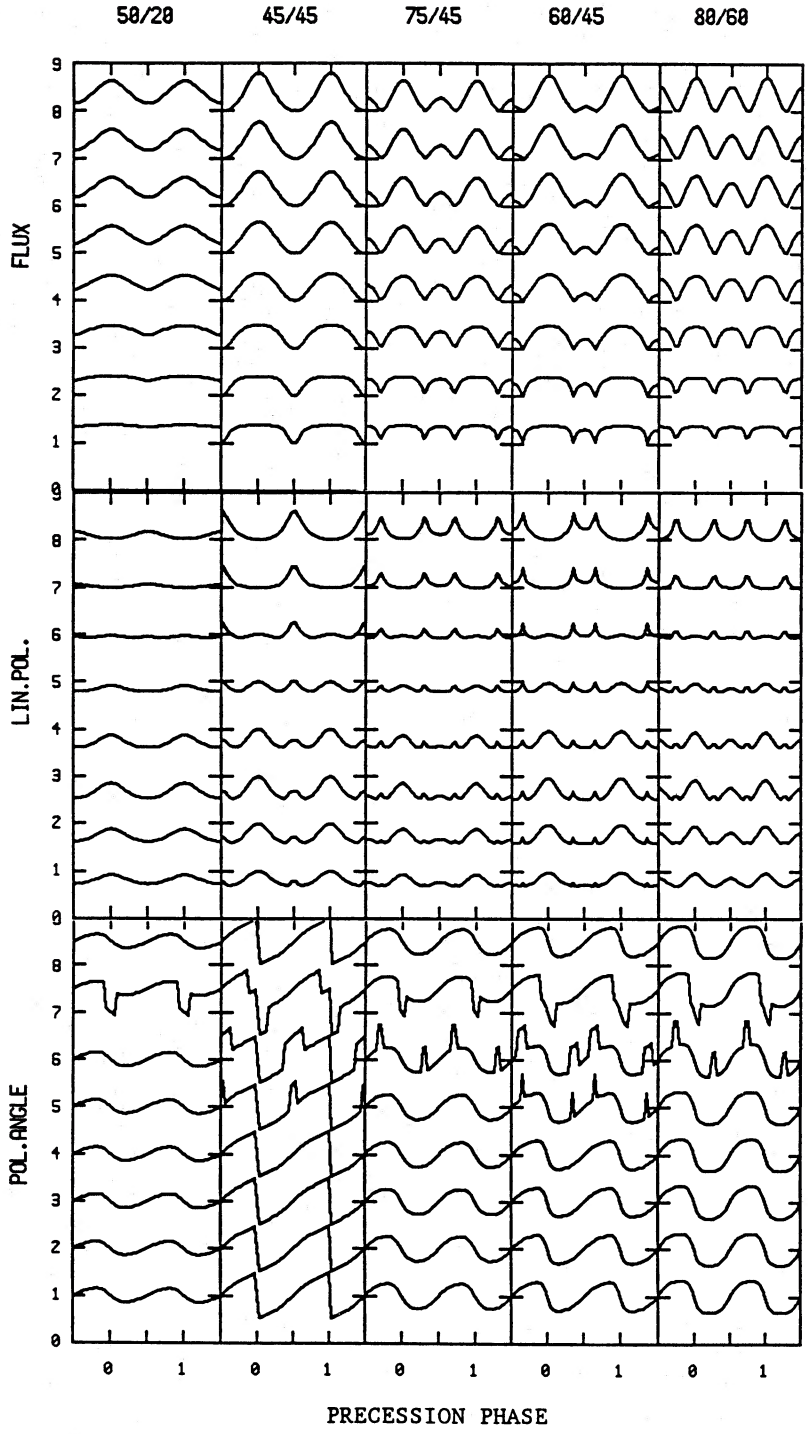

FIG. 5.—Accretion disk of $\tau_0 = 2$ viewed at different angles (phase), also applicable to precessing disk. (*top panels*) Normalized flux amplitude. (*middle panels*) Linear polarization $P_L(\%)$, with value zero at the left tick mark for that curve or depth, going from plus 20% (one tick mark above) to −20% (one tick mark below). *lower panels* Position angle of the electric vector respect to the sky projection of the fixed system angular momentum vector, zero at the left tick mark for each curve or depth, going from from +180 at the tick mark above, to −180 degrees at the tick mark below. The numbers along the top give the aspect angles (see text), and the abscissa is the precession phase. Each panel shows eight curves, corresponding from bottom to top to the eight increasing disk thicknesses of Fig. 4.

process, which could be easily verified by X-ray polarimetry. The impact of such techniques on our understanding of SN 187A, of enormous actual interest, could be very large indeed. The mechanism of X-ray and gamma-ray emission of the radio pulsars themselves, however, is likely to be more complicated. The observation of optical polarization in two radio pulsars, and the similarity of the radio and X-ray spectral indices have suggested a similar synchrotron origin, which predicts the X-rays to be polarized in the same direction as the optical radiation (e.g., Zheleznyakov and Shaposhnikov 1972). Other models invoke curvature radiation from coherent bunches of relativistic electrons, while the X-rays would still be synchrotron, in which case the optical and X-ray radiation polarization would be orthogonal (e.g., Sturrock Petrosian, and Turk 1975). More recent models involve slot-gaps (e.g., Arons 1982) or outer gaps (Cheng, Ho and Ruderman 1986) and radiation by pair cascades (e.g., Daugherty and Harding 1982). X-ray polarimetry would be a key discriminant among the various models being considered. Furthermore, the degree of beaming would affect the angle and degree of polarization. Since the degree of beaming is one of the key uncertainties in statistical population studies of pulsars, which bear directly on the question of the total rate of neutron star formation and supernova rate, an elucidation of the pulsar radiation physics has far-reaching implications for stellar and galactic evolution as well.

Extragalactic X-ray polarimetry, while requiring larger instruments (but no larger than AXAF or XMM) or longer observing times on the smaller missions, could bring some of the richest rewards. Quasars and AGNs emit much of their radiation in X-rays, and this radiation is more likely to originate in the neighborhood of the central engine (Rees 1984). There is no consensus on whether this radiation is thermal, or nonthermal, nor indeed is it clear whether the radiation arises from disk, a torus, a quasi-spherical flow, or a jet. As emphasized in § I and elsewhere (Phinney 1983; Mészáros 1984), spectral and timing predictions of many of these physically so different models can, and do, mimic each other in this restricted two-parameter phase space of frequency and time. However, the polarization predictions from the various models are widely different (e.g., Begelman and McKee 1983; Phillips and Mészáros 1986; Begelman and Sikora 1987) ranging from less than a few percent (spherical), through 2%–10% (disks; see § III), to greater than 10%–20% (jets). Discriminating between models by means of the polarization would not only settle many issues of quasar physics, but would also bear directly on several cosmological issues. For instance, in the case of disks and even more of jets, the X-ray polarization would depend on the beaming, which can be of far-reaching consequences for quasar population density studies, and therefore for such things as determining the Hubble constant.

V. OBSERVATIONAL PROSPECTS

Two different types of polarimeters have been flown to date: Bragg crystal devices and scattering devices. Bragg crystal polarimeters are based on the fact, that at a Bragg angle of 45° crystals only reflect (diffract) radiation which is polarized perpendicular to the plane of incidence. The advantage of this type of device is that it is small and can be used at the focus of a grazing incidence telescope, to increase the number of photons collected. One drawback is that the energy response of a Bragg crystal is limited to narrow bands centered on the photon energies that correspond to the different diffraction orders that satisfy the Bragg condition at 45°. Typical photon energies are a few keV, and typical widths are about 3 eV. Scattering devices depend on the fact that the electron scattering cross section for polarized radiation is anisotropic in the plane normal to the direction of the incident photon. Scattering polarimeters have the advantage that they can measure polarization as a function of energy from a lower photon energy set by photoelectric absorption in the material (typically 8 or 10 keV) to an upper limit set by the dropoff in the source flux, where the detector signal is dominated by background effects. Only a very small scattering detector would fit at the focus of a grazing incidence collector, and in order to achieve a polarization sensitivity of 1% in 1 day from a large collection of sources, the collecting area required is of the order of 1000 cm^2. This is an optical system of the class being considered for AXAF or XMM, and could be easily incorporated at a (relatively) low cost into such missions. While the detection of X-ray polarization is clearly achievable in such missions, a much more modest experiment would also be able to measure X-ray polarization in a large number of sources. We discuss both of these possibilities below, starting with the most immediately feasible one.

We first consider a prototype for a small-satellite instrument based on a scattering device of novel design, which does not require a grazing incidence collector. Such a device can be launched by a Scout rocket and would be well suited to the study of a large number of galactic compact X-ray sources at energies above 10 keV. The geometry of the X-ray scatterer is that of a thin disk. The disk thickness is chosen to be a fraction of a scattering length, which avoids the problem of multiple scatters within the disk that would tend to confuse the polarization information of the first scattering event. The diameter, on the other hand, is limited only by the dimensions of the spacecraft. This configuration permits an arbitrarily large collection area, which compensates for any low fluxes and/or weak polarization in the source. A low atomic weight scattering material (beryllium) is chosen to give a low photoabsorption threshold. The detection system is an array of proportional counters arranged in a cylinder or polygonal prism, with the disk located coaxially at the midplane of the detector array (Fig. 6). Photons enter along the direction of the axis of the instrument, which is provided with a collimator to reduce the contribution of the diffuse background. Polarization manifests itself as an azimuthal variation of the X-ray flux entering the counter. In order to avoid a number of systematical errors, the polarimeter and the spacecraft could be rotated slowly (~ 1 RPM) about the line of sight to the X-ray source. In this case the polarization produces a modulation of the count rate in each detector element. The amplitude of the modulation is directly related to the degree of polarization. To achieve a high level of background rejection, the proportional counters could have a multilayer structure, with an inner propane layer capable of vetoing charge particle events, and an outer anticoincidence layer shielding the instruments from recoil electron produced by background gamma rays. An imaging proportional counter filled with xenon can be used to detect the X-rays scattered by the beryllium disk. Such a scattering polarimeter would have a polarization sensitivity of about 2% at the 99% confidence level for Her X-1 in a 2 keV band at 15 keV with an observing time of 2×10^5 s, a sensitivity increase of a factor ~ 100 over the best X-ray polarimeter flown to date. In the important case of Cyg X-1, the minimum detectable polarization (99% confidence level) would be $\sim 0.5\%$ for an observing time of 2×10^5 s for the entire 10–20 keV band. This

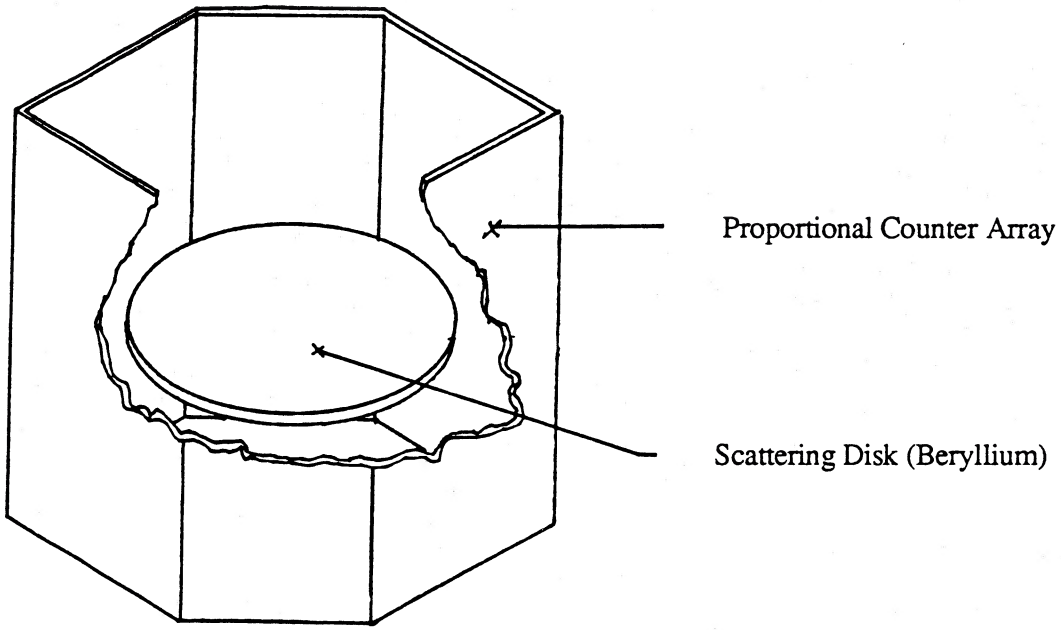

FIG. 6.—Diagram of a low-cost scattering X-ray polarimeter, which could be launched into orbit by a Scout rocket for the detection of galactic X-ray sources at high energies. See text for details.

instrument could make useful measurements on at least 50 other known galactic sources and would fit into a spacecraft that can be launched on a Scout rocket, a reliable and relatively inexpensive launcher.

To exploit to its fullest extent the major advantages offered by X-ray polarimetry, and to detect both extragalactic and galactic sources, an initial exploratory mission (such as a Scout launched device discussed above) could be followed up with a larger scale experiment, flown in one of the large missions of the next decade. To include a polarimeter in one of these may be one of the better ways of getting a large return for a moderate investment, in view of the significant and far-reaching astrophysical issues that it can address. Among these are the elucidation of the mechanism of AGNs, with its related cosmological implications, a fuller understanding of the SN remnants in our galaxy and in the LMC, and the physical study of extragalactic and galactic compact sources. Various designs are possible (e.g. Garmire, 1987). Here we discuss the possibility of a larger polarimeter sytem, combining a photon collector with a versatile focal plane detector which would be suitable for AXAF or for the European Space Agency's XMM satellite (Novick, Chanan, and Helfand 1985). For maximum efficiency at various energies and maximum usefulness on different types of targets, one could build an instrument which exploits both of the previously mentioned polarimetry techniques. Such a multi-spectral-polarimeter would combine the high sensitivity of a number of Bragg crystals in several different narrow wavebands ($\Delta E/E < 0.1$) disposed between 0.26 keV and 7.8 keV with the broad-band ($\Delta E/E \approx 0.2$) capabilities of a lithium scattering device between 4 to upwards of 10 keV. A sketch of such a hypothetical instrument is shown in Figure 7. The entire assembly rotates about the optical axis, and polarization manifests itself as a modulation of the detected signal at twice the rotation frequency. Two multiwire imaging proportional counters located on opposite sides of the rotating platform detect the scattered X-rays, tagging each photon with x and y position, time and energy information. This polarimeter system would be able to measure in the 0.26 keV band with 99% confidence a 2% degree of polarization in the Seyfert 1 Mrk 335 or a 6% polarization in the quasar 3C 273 in an observation time of 10^5 s duration, and a 2% polarization in the Seyferts 1 Mrk 509 and ESO 141–G55 in 2×10^5 s. It could measure, in the same band and similar observing times, down to 0.7% polarization in the BL Lac objects Mrk 421, Mrk 501, PKS 2155−304 and PKS 058−22. It would in addition be able to detect polarization down to 1%–2% at higher energies in these or other AGNs with somewhat longer observing times, and down to similar polarization levels in a large number of galactic sources (accretion-powered and rotation-powered pulsars, X-rays bursters, galactic bulge sources, supernova remnants, galactic black hole candidates, cf. above) in observing times of $1–3 \times 10^5$ s.

In conclusion, one can say that X-ray polarimetry is an extremely attractive and so far unexploited observational technique, which could lead to the acquisition of a large amount of qualitatively new data of potentially far reaching astrophysical significance.

This research has been supported in part through NSF grant AST 8514735 to Penn State University, and NASA contract NAG 5-618 to Columbia Astrophysics Laboratory.

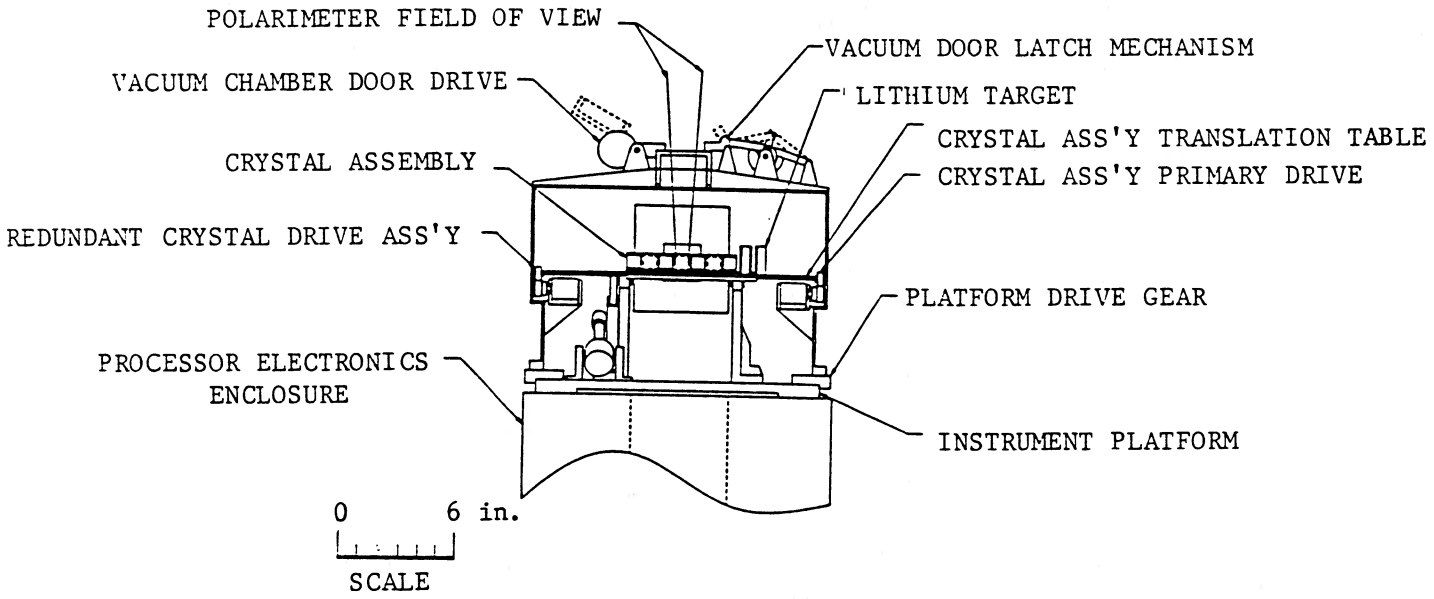

FIG. 7.—Diagram of a multispectral polarimeter, using both Bragg crystals and a scattering device, which could operate at the focal plane of a facility such as the XMM observatory. This would be able to detect both galactic and extragalactic X-ray sources with a high sensitivity.

REFERENCES

Angel, J. R. P. 1969, *Ap. J.*, **158**, 219.
Arons, J. 1983, *Ap. J.*, **266**, 215.
Bardeen, J., and Peterson, J. A. 1975, *Ap. J.* (*Letters*), **195**, L65.
Begelman, M. C., and McKee, C. F. 1983, *Ap. J.*, **257**, 318.
Begelman, M. C., and Sikora, M. 1987, *Ap. J.*, **322**, 650.
Bussard, R. W., Lamb, F. K., and Pakey, D. 1987, preprint.
Bussard, R. W., Mészáros, P., and Alexander, S. 1985, *Ap. J.*, **297**, L21.
Canuto, V., Lodenquai, J., and Ruderman, M. 1971, *Phys. Rev.*, **D3**, 2303.
Chanan, G. A., Novick, R., and Silver, E. H. 1979, *Ap. J.* (*Letters*), **228**, L71.
Cheng, A., Ho, C., and Ruderman, M. A. 1986, *Ap. J.*, **300**, 522.
Connors, P. A., Piran, T., and Stark, R. F. 1980, *Ap. J.*, **235**, 224.
Cunningham, C. T. 1976, *Ap. J.*, **208**, 534.
Daugherty, J. K., and Harding, A. K. 1982, *Ap. J.*, **252**, 337.
Garmire, G. 1979, private communication.
Gnedin, Yu. N., and Sunyaev, R. A. 1974, *Astr. Ap.*, **36**, 379.
Gnedin, Yu. N., and Pavlov, G. G. 1974, *Soviet Phys.—JEPT*, **38**, 903.
Gnedin, Yu. N., Pavlov, G. G., and Shibanov, Yu. A. 1978*a*, *Soviet Phys—JETP Letters*, **27**, 305.
———. 1978*b*, *Sov. Astr.* (*Letters*), **4**, 117.
Grindlay, J. E. 1985, in *Galactic and Extraglactic Compact X-ray Sources*, ed. Y. Tanaka and W. Lewin (Tokyo: Institute of Space and Astr. Sci), 215.
Helfand, D. 1984, *Adv. Space Res.*, Vol **3**, Nos 10–12, p. 29.
Herold, H., Ruder, H., and Wunner, G. 1981, *Plasma Phys.*, **23**, 775.
Katz, J. I. 1973, *Nature*, **246**, 87.
Kirk, J. G. 1980, *Plasma Phys.*, **22**, 639.
Lapidus, I. I., and Sunyaev, R. A. 1985, *M.N.R.A.S.*, **217**, 291.
Lightman, A. P., and Shapiro, S. L. 1975, *Ap. J.* (*Letters*), **198**, L73.
Mészáros, P. 1984, in *Non-thermal and Very High Temperature Phenomena in X-ray Astronomy*, ed. G. Perola and M. Salvati, (Rome: University of Rome Press, Italy), p. 33.
Mészáros, P., and Nagel, W. 1985*a*, *Ap. J.*, **298**, 147.
———. 1985*b*, *Ap. J.*, **299**, 138.
Mészáros, P., and Ventura, J. 1978, *Phys. Rev.* (*Letters*), **41**, 1544.
———. 1979, *Phys. Rev. D.*, **19**, 3565.
Nagel, W. 1981, *Ap. J.*, **251**, 288.
Novick, R., *et al.* 1972, *Ap. J.* (*Letters*), **174**, L1.
Novick, R., Chanan, G., and Helfand, D. 1985, in *Cosmic X-ray Spectroscopy Mission*, (Paris: European Space Agency) (ESA SP-239) p. 265.
Pavlov, G. G., and Shibanov, Yu. A. 1979, *Soviet Phys.—JETP*, **49**, 741.
Pavlov, G. G., Shibanov, Yu. A., and Yakovlev, D. G. 1980, *Ap. Space Sci.*, **73**, 33.
Petterson, J. A. 1975, *Ap. J.* (*Letters*), **201**, L61.
Phillips, K. C. and Mészáros, P. 1986, *Ap. J.*, **310**, 284.
Phinney, S. 1983, Ph.D. thesis, Cambridge University.
Pineault, S. 1977, *M.N.R.A.S.*, **179**, 691.
Priedhorsky, W., and Terrell, J. 1984, *Ap. J.* (*Letters*), **284**, L17.
Rees, M. J. 1975, *M.N.R.A.S.*, **171**, 457.
———. 1984, *Ann. Rev. Astr. Ap.*, **22**, 471.
Riffert, H., and Mészáros, P. 1988, *Ap. J.*, in press.
Roberts, W. J. 1974, *Ap. J.*, **187**, 575.
Silver, E. H., *et al.* 1978. *Ap. J.*, **225**, 221.
———. 1979, *Ap. J.*, **232**, 248.
Soffel, M., *et al.* 1983, *Astr. Ap.*, **126**, 251.
Stark, R. F., and Connors, P. A. 1977, *Nature*, **266**, 429.
Sturrock, P. A., Petrosian, V., and Turk, J. S. 1975, *Ap. J.*, **196**, 73.
Sunyaev, R. A., and Titarchuk, L. G. 1985, *Astr. Ap.*, **143**, 374.
Taylor, J. H., and Stinebring, D. R. 1986, *Ann. Rev. Astr. Ap.*, **24**, 285.
Truemper, J., *et al.* 1986, *Ap. J.* (*Letters*) **300**, L63.
Weisskopf, M. C., *et al.* 1976, *Ap. J.* (*Letters*), **202**, L77.
———. 1978, *Ap. J.* (*Letters*), **220**, L117.
White, N. E., and Holt, S. S. 1982, *Ap. J.*, **257**, 318.
Zheleznyakov, V. V., and Shaposhnikov, U. E. 1972, *Ap. Space. Sci.*, **18**, 141.

G. A. CHANAN: Department of Physics, University of California-Irvine, Irvine, CA 92717

P. MÉSZÁROS: The Pennsylvania State University, Department of Astronomy, 525 Davey Laboratory, University Park, PA 116802

R. NOVICK AND A. SZENTGYÖRGYI: Department of Physics, Columbia University, 528 West 120th Street, New York, NY 10027

M. C. WEISSKOPF: Code ES-62, NASA/Marshall Space Flight Center, Huntsville, AL 25812